Detailed distinct element modeling of a Utrecht wharf cellar for the assessment of the load-bearing capacity and failure mechanism

Oktiovan, Y.P.; Messali, F.; Rots, J.G.

DOI
10.4203/ccc.6.6.2

Publication date
2023

Document Version
Final published version

Published in
Proceedings of the Seventeenth International Conference on Civil, Structural and Environmental Engineering Computing

Proceedings of the Seventeenth International Conference on
Civil, Structural and Environmental Engineering Computing
Edited by: P. Iványi, J. Kruis and B.H.V. Topping
Civil-Comp Conferences, Volume 6, Paper 6.2
Civil-Comp Press, Edinburgh, United Kingdom, 2023
doi: 10.4203/ccc.6.6.2

Detailed distinct element modeling of a Utrecht wharf cellar for the assessment of the load-bearing capacity and failure mechanism

Y.P. Oktiovan, F. Messali and J. Rots

**Faculty of Civil Engineering and Geosciences,
Delft University of Technology, Delft, Netherlands**

Abstract

The city of Utrecht is famously known for the system of canals and the wharf cellars integrated to the heart of the city, whose construction dates back to the 1300s. Due to increased traffic volume which caused the increase in dead load and traffic load, it is important to assess the safety and state of maintenance of these historical structures. In this paper, a safety assessment framework for wharf cellars is introduced and the application to a wharf cellar as a case study in central Utrecht is provided. The geometry of the wharf cellar is parametrically generated and used for the numerical analysis using the distinct element method (DEM), where arch units and piers are modeled as discrete blocks separated by zero-thickness interfaces. Traffic load models in accordance with the Dutch guideline for emergency vehicles are calculated. Unlike traditional approaches, the three-dimensional load distribution through the soil is modeled. The structure's compliance with this load is assessed, and the failure load and mechanism are observed. The analysis result can be used to help engineers on providing insights into the safety and stability of the cellars in an effort to extend the lifespan of the historical structures.

Keywords: Utrecht wharf cellar, distinct element method, 3DEC, traffic load, barrel vault, Boussinesq distribution, safety assessment

1 Introduction

Masonry arches have been extensively used since the realization of the potential of arches for bridge construction by the Romans [1]. In the Netherlands, builders have been using arches and vaults since the Medieval Age, specifically in the city of Utrecht. Between the 1300s and 1500s, the merchants in Utrecht dug out tunnels to build cellars at the wharf level of the city canal to store goods. These tunnels were connected to the canal houses at street level and extended to the public road system.

An example of a wharf cellar and the schematics of the cellar components are presented in Figure 1a and 1b, respectively. A typical cellar system comprises a longitudinal bond barrel vault, cross bond masonry piers interconnected to adjacent wharf cellars, and a spandrel wall for the façade. Due to urbanization and increased traffic volume, the sustained load changed from horses and carriages to motorized vehicles. Furthermore, the recent collapse of historic properties across the Netherlands, such as the collapse of quay walls in Amsterdam [2], shed light on the importance of safety assessment of historical structures and infrastructures in Dutch cities.

(a) Real world footage. (b) Cellar schematics.

Figure 1: Example of a wharf cellar in Utrecht.

In this context, this paper introduces a safety assessment framework based on the distinct element modeling (DEM) strategy and uses the framework for the assessment of a Utrecht wharf cellar as a case study. The compliance of the structure is checked against the load model by the Dutch Guideline for traffic loads on bridges and other civil engineering works [3]. If the structure is compliant, the applied load is increased until failure of the cellar is achieved.

2 Case Study of The Utrecht Wharf Cellar

The cellars used for the case study are located in the *Kromme Nieuwegracht* canal. Information pertaining to the geometrical and material of the case study can be found

on the investigation report conducted by Royal Haskoning DHV [4], hereby termed as the investigation report. The cellar system consists of three inter-connected barrel vaults and load-bearing piers with varied springing levels, as shown in Figure 2. The cellar heights are measured based on the NAL (Normal Amsterdam Level / *Normaal Amsterdams Pell*, a reference plane for height in the Netherlands. The foundations of the cellar are shallow foundations made out of masonry sitting on loose sand.

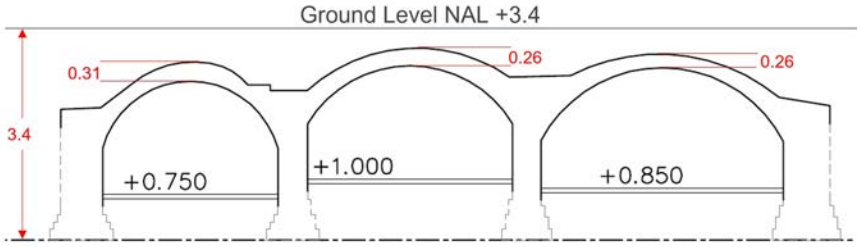

Figure 2: Cross-section of a wharf cellar in *Kromme Nieuwegracht* (units in m).

The cellar system's total span is approximately $13\,\mathrm{m}$ long with $4.8\,\mathrm{m}$ depth and comprises three arches whose span ranges from $2.4\,\mathrm{m}$ to $4.0\,\mathrm{m}$, as well as load-bearing piers whose height varies from $2.4\,\mathrm{m}$ to $2.6\,\mathrm{m}$. Finishing layers were found at the top- and bottom-side of the cellar, with an additional bituminous layer for waterproofing at the top-side arch. The backfill of the cellar system consists of loosely packed sand with clinker pavement on top of it. The density of the soil and pavement is taken as $18\,\mathrm{kN\,m^{-3}}$ and $23\,\mathrm{kN\,m^{-3}}$, respectively. Similar to the clinker pavement, the density of the masonry unit is taken at $23\,\mathrm{kN\,m^{-3}}$. The necessary material properties for the numerical modeling are shown in Table 1.

Properties	Table F.2. NPR9998(2020)	Masonry Clay Brickwork (pre-1945)	Units
Elastic modulus	E_m	6000	$\mathrm{N\,mm^{-2}}$
Shear modulus	G_m	2500	$\mathrm{N\,mm^{-2}}$
Uniaxial tensile strength	$f_{ma;b;per}$	0.1	$\mathrm{N\,mm^{-2}}$
Initial shear strength	$f_{ma;v;0}$	0.3	$\mathrm{N\,mm^{-2}}$
Shear friction coefficient	$\mu_{ma;m}$	0.75	[-]

Table 1: Masonry material properties as per Table F.2 of NPR9998 [4].

The material properties of the masonry elements are based on the characteristic values specified in Table F.2 of NPR 9998+C1:2020 [5]. The dilatancy angle is assumed to be zero. The cross-section of the barrel vault was obtained by drilling two boreholes at the highest point of the middle arch. Based on the drill core, the cellar arch comprised one brick unit stacked vertically with dimensions of 220x110x55 ($\mathrm{mm^3}$ (L x W x H) and an additional unit stacked horizontally, with a mortar thickness of 10mm.

(a) Arch (b) Pier

Figure 3: Investigation photos of the wharf cellar bond pattern.

The investigation photos of the bond pattern on the arch and pier sections of the cellar are shown in Figures 3a and 3b, respectively. A cross-bond pattern was found at the piers while a longitudinal header bond pattern was found at the arches.

3 Modeling Strategies

The safety assessment of the wharf cellar under traffic load is conducted using the three-dimensional DEM [6] software called *3DEC* [7]. The numerical method has been used extensively for the numerical analysis of masonry structures and, in this case, is useful to identify the post-peak response and failure mechanism of the cellar system. Masonry blocks in DEM are modeled discretely as assemblages of rigid or deformable blocks with deformable contact points at their discontinuities, governed by stiffness in normal and tangential directions. Equilibrium in DEM is achieved by solving the equation of motion using an explicit time-marching scheme.

3.1 Model description

The process of the safety assessment begins with the generation of the cellar system geometry using a parametric design tool called *Rhino+Grasshopper* using the inputs from Figure 2. The geometry generation tool contains C# scripts for fast and robust design of the vaulted masonry units. The discretization of the case study model is shown in Figure 4. masonry units are modeled with extended dimensions to account for half of the mortar joint thickness on all sides. For the sake of modeling simplicity, the crown height of each arch is made uniform. The faithful representation of the case study will be considered as a future improvement to this framework. To retain the face-to-face contact between the vertically and horizontally stacked units, the horizontal units are discretized into three elements, corresponding to the units underneath them.

The discretization of the cellar piers and extended sections towards the $\frac{1}{4}$-height of the arch is presented in Figure 5. The cross bond pattern at the cellar piers is faithfully modeled where header bond with additional queen closer is used for the odd course

while stretcher bond is applied to the even course. However, the bond pattern changed from the springing level to the $\frac{1}{4}$-height of the arch, where a running stretcher bond pattern is used with alternating stretcher and header towards the depth of the cellar.

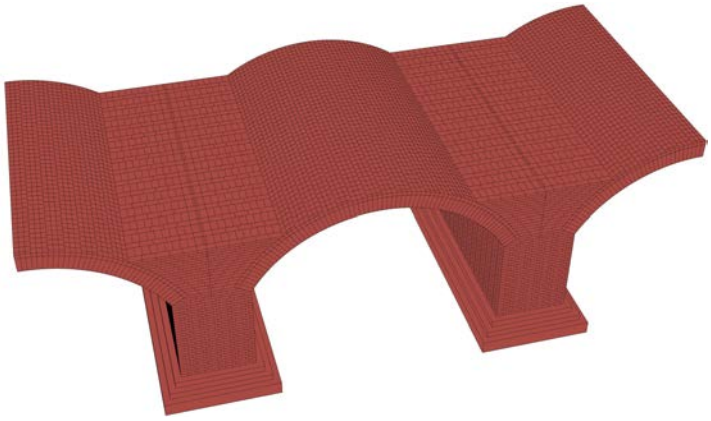

Figure 4: Discretization of a Utrecht wharf cellar.

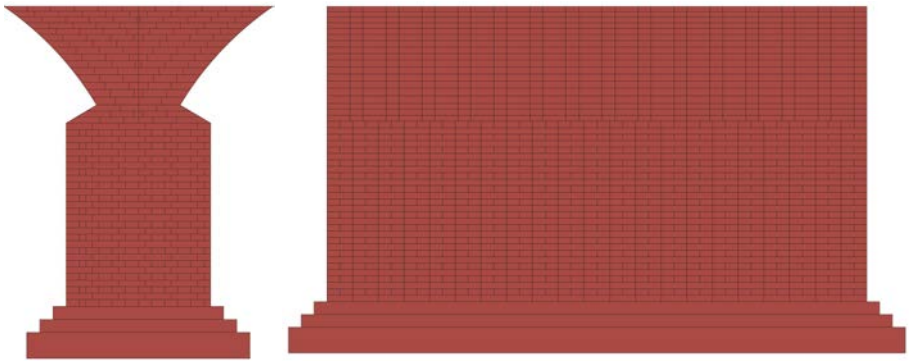

(a) Front view. (b) Leftside view.

Figure 5: Discretization of the cellar piers.

The blocks are then imported to *3DEC* where blocks are modeled as rigid blocks. Since deformations are lumped at the discontinuities/joints, the use of rigid blocks is sufficient enough for the case of the safety assessment of masonry structures. A Coulomb friction joint constitutive model is applied to the contacts with Table 1 as the input parameters. The normal k_n and shear k_s stiffnesses at the contacting joints are defined as a function of Young's moduli of brick units and mortar spread over the contact area, shown in Equation (1). The unit of the stiffnesses is in $\mathrm{MPa\,mm^{-1}}$.

$$k_n = \frac{E_b \cdot E_m}{(E_b - E_m) \cdot h_j} \quad \text{and} \quad k_s = \frac{k_n}{2(1+v)} \tag{1}$$

where E_b and E_m are the brick and mortar Young's moduli,respectively, h_j is the joint height and v is the Poisson's ratio, set to 0.2. The mortar joint properties are empirically obtained based on the work of [8].

3.2 Boundary and loading conditions

As shown in Figure 4, only half of the left- and right-side arches are modeled to save computational time. The bottom-most of both piers are fixed and to simulate the symmetric conditions at both ends of the arches, non-physical rigid blocks are attached to the arches with frictionless contacts between the blocks and the vault elements.

Once the material properties are defined, the numerical model is brought to equilibrium under gravity load, and then the backfill above the cellar is added as dead load and also brought to equilibrium. The traffic load is defined in accordance with the Load Model 3 of the NEN-EN 1991-2/NB guideline [3], hereby termed as the Dutch guideline, and implemented. The load model corresponds to the fatigue life assessment check for bridges subjected to emergency vehicle loads such as ambulance or fire brigade trucks.

The traffic load is incrementally applied until the full application of the load, termed the normative load. If the maximum vertical displacement of the structure is still within the specified threshold by the Dutch guideline, in this case, equals to $0.032\,\mathrm{m}$, the structure is considered compliant with the normative load. After this sequence, the traffic load is applied considering the increasing Load Multiplier (LM) until the failure of the arch occurs.

The backfill soil is not explicitly defined in this model, and instead is replaced as a dead load distributed over the cellar top surface. Similarly, the traffic load is applied as a distributed load. Following the assumption of Boussinesq solution where a semi-infinite elastic soil exists below the surface of the applied load, Frazee [9] proposed closed-form solutions for three-dimensional finite area load of the Boussinesq solution, in accordance to the Cartesian coordinates of the evaluated point. The 3-D Boussinesq solution for finite area load is given in Equation (2a). Point a,b,c, and d in Equation (2b) correspond to each corner of the finite area load. Readers are referred to Frazee [9] for the order of the corners. The coordinates for each corner are then applied to Equation (2b) by substituting β and δ for the corresponding corners.

$$q_v(x,y) = \frac{q}{2\pi}[f(b,d) - f(a,d) - f(b,c) + f(a,c)] \tag{2a}$$

where

$$\begin{aligned} f(\beta,\delta) = {} & \frac{z(\beta-x)(\delta-y)\left[(\beta-x)^2+(\delta-y)^2+2z^2\right]}{\left[(\beta-x)^2+z^2\right]\left[(\delta-y)^2+z^2\right]\sqrt{(\beta-x)^2+(\delta-y)^2+z^2}} \\ & + \arctan\left[\frac{(\beta-x)(\delta-y)}{z\sqrt{(\beta-x)^2+(\delta-y)^2+z^2}}\right] \end{aligned} \tag{2b}$$

The Boussinseq load distribution is implemented within a specified angle of dispersion limit. According to Chapter 4.9.1 of the Dutch guideline [3], the traffic load dispersion along the arch ring is limited by an angle of 30° both in the longitudinal and transversal directions of the arch. The Load Model 3 in accordance with Dutch

guideline [3] is based on a traffic load in the case of emergency vehicle services. The ladder fire brigade truck is chosen for the assessment in this paper as it has the heaviest axle load weight. The tire contact area for this paper is defined as $0.447 \times 0.1225\,\mathrm{mm}$. The ladder truck has a load of $40\,\mathrm{kN}$ per tire for the front axle tires and $50\,\mathrm{kN}$ for the back axle tires. Furthermore, according to the Dutch guideline [3], a magnification factor of 1.4 must be considered when the special vehicles move at a speed of more than $5\,\mathrm{km\,h^{-1}}$ to account for the dynamic effects imposed to the arched structures.

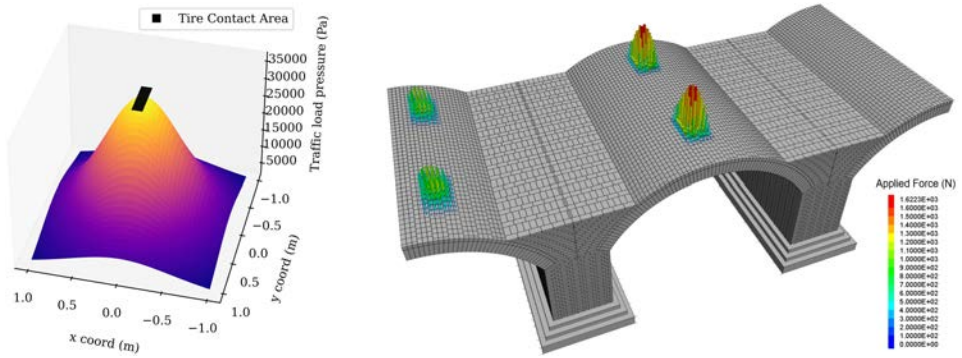

(a) Tire contact pressure (b) Implementation in 3DEC

Figure 6: Illustration of the implementation of traffic load dispersion in 3DEC

The implementation of Equation (2) using the back axle tire load (including dynamic magnification factor) and the aforementioned tire contact area is presented in Figure 6a. The vehicle load position was chosen from the most unfavorable position identified by the investigation report [4]. It was found that the most unfavorable position was when the back axle load was placed at the center of the middle cellar and the front axle was placed $4.2\,\mathrm{m}$ towards the left-side arch by the direction of travel. The implementation in *3DEC* is shown in Figure 6b.

4 Numerical Analysis Results

In this section, the results from the quasi-static analysis of the DEM model are presented. Results are shown in terms of vertical displacements, normal joint displacement, compressive normal stress, damaged state, and deformed shape of the cellar.

4.1 Safety assessment under normative load

The quasi-static analysis for the normative load was successfully conducted with little to no damage found on the cellar system. The evolution of the numerical model in terms of vertical displacement (d_z), maximum normal joint displacement ($\delta_{n,tens}$), and maximum compressive normal stress ($\sigma_{n,max,comp}$) is presented in Table 2.

Compressive stress is assumed to be positive. At the normative load of LM1, the

Load Multiplier	d_z mm	$\delta_{n,tens}$ mm	$\sigma_{n,max,comp}$ MPa	Notes
LM0	-0.089	0.006	0.547	After overburden load is applied
LM1	-0.159	0.016	0.907	

Table 2: Responses of the wharf cellar under backfill overburden and normative loads.

maximum vertical displacement observed after the full normative load was applied is still below the threshold displacement set by the Dutch guideline. Separation at the bottom-side of the middle arch occurred, with maximum normal joint displacement shown in Table 2. It is observed as well that at the full application of the normative load, the maximum compressive stress found at the arch was still lower than the compressive strength defined in Table F.2 of NPR 9998+C1:2020 [5], which is $8.5\,\mathrm{MPa}$.

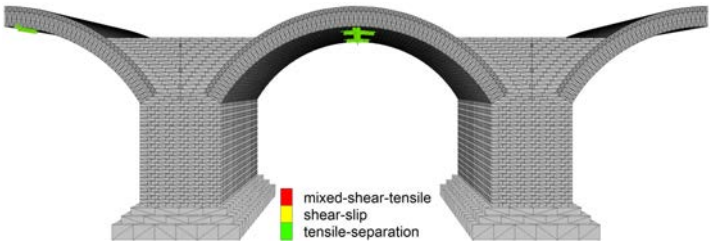

Figure 7: Damaged state at middle arch after full application of normative load.

The separation is indicated by the presence of tensile damage shown in Figure 7. Comparing the maximum vertical displacement against the threshold, it is concluded that the cellar system is compliant under the normative load model 3 according to the Dutch guideline [3] at the most unfavorable position within the wharf cellar system.

4.2 Assessment of the failure load and failure mechanism

Failure in the quasi-static analysis under DEM occurs when the ratio of monitored out-of-balance forces versus internal forces flatlined at an arbitrarily high value. The failure of the cellar system under Load Model 3 of the Dutch guideline was observed at Load Multiplier 7 (LM7), with d_z of $-0.897\,\mathrm{mm}$, $\delta_{n,tens}$ of $0.556\,\mathrm{mm}$, and $\sigma_{n,max,comp}$ of $4.978\,\mathrm{MPa}$. The damaged state of the cellar system at failure is presented in Figure 8. At failure, multi-ring separation was observed between the horizontal and vertical arch units on the middle and left-side arches as well as uplift on the right-side arch due to extreme compression on the other arch counterparts.

Furthermore, due to significant pressure at the tire load areas, which is highlighted in Figure 8 by blue and pink shades for back and front tire loads, respectively, the section of the arch in-between the tire contact areas experienced tensile damage on both horizontal and vertical arch units.

The deformed shape of the cellar is shown in Figure 9, magnified by a factor of

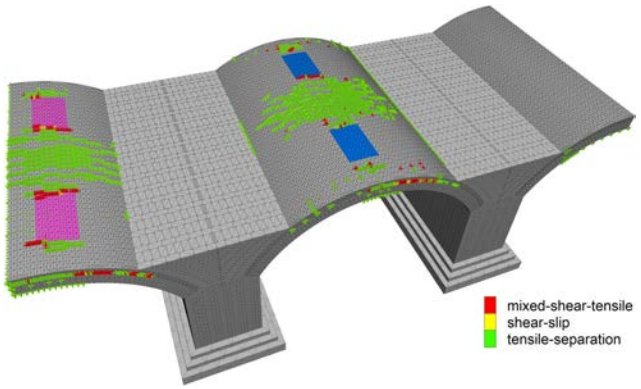

Figure 8: Damaged state of the cellar at failure load.

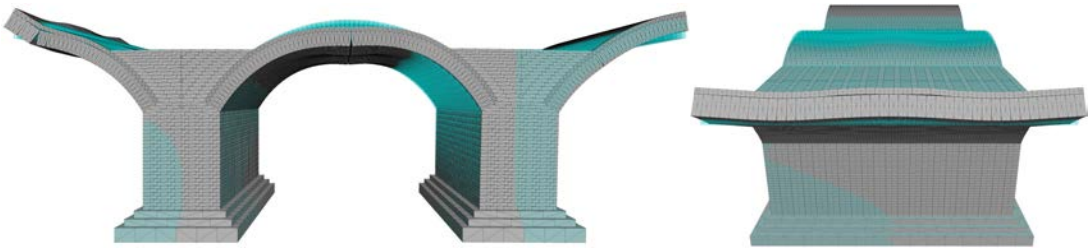

(a) Front view (b) Side view

Figure 9: Deformed shape of the cellar model at failure load.

50. The undeformed configuration is shown in a blue transparent shade. From the front view in Figure 9a, the separation occurred at the left and middle arch units. Uplift of the right-side arch due to the extreme compression on the other arches is also depicted. From the side view shown in Figure 9b, the multi-ring separation at the region in-between the tire contact area can be visualized, with localized compressive forces at the tire contact areas forming a sinusoidal-like deformation of the cellar arch.

5 Conclusions

In this paper, a DEM-based numerical approach is introduced for the safety assessment of the masonry wharf cellar structure located in the city of Utrecht. A rigid block DEM model is used where all deformations and nonlinearities are lumped at the block discontinuities. Traffic load is implemented by using a three-dimensional load dispersion model according to the Boussinesq distribution and load in accordance with the Dutch guideline is investigated at the most unfavorable position.

This exploratory study on the potential of DEM for studying wharf cellars in Utrecht appeared to be able to predict a failure mechanism and failure load in a stable and robust manner, without any convergence issues. The results appeared to be reasonable from the physical point of view, but validation and cross-comparison against different assessment method is needed. With the current assumptions, it was observed that there was a hidden reserve of load-bearing capacity for the wharf cellar system where the cellar was still able to sustain a traffic load of up to 7 times the normative Load

Model 3 according to the Dutch guideline.

This was the first exploratory study into the potential of using DEM for structural analysis of Utrecht wharf cellars. Validation in the form of experiments and comparison to other methods typically used to evaluate failure load and mechanism such as limit analysis will be performed to confirm this finding. Also, comparisons between the current DEM and FEM analyses are planned to be performed from the perspective of stability on the solution procedures, robustness, and accuracy of the constitutive models as well as discretization aspects involved. Different positions and load models, sensitivity analysis on the material parameters, effect of pre-damage on the ultimate limit state, and the faithful representation of the arch height in each section will be considered as part of the future work of this paper.

References

[1] V. Sarhosis, S. De Santis, G. de Felice, "A review of experimental investigations and assessment methods for masonry arch bridges", Structure and Infrastructure Engineering, 12, 1439-1464, 2016, DOI: 10.1080/15732479.2015.1136655

[2] S. Sharma, M. Longo, F. Messali, "A novel tier-based numerical analysis procedure for the structural assessment of masonry quay walls under traffic loads", Frontiers in Built Environment, 9, 1-17, 2023, DOI: 10.3389/fbuil.2023.1194658

[3] NEN-EN 1991-2:2021, "Eurocode 1 - Actions on structures - Part 2: Traffic loads on bridges and other civil engineering works", European Committee for Standardization, 2021.

[4] Royal Haskoning DHV, "Verificatieberekening kelder Kromme Nieuwegracht te Utrecht", Royal Haskoning DHV, 2021.

[5] NPR 9998:2020, "Assessment of structural safety of buildings in case of erection, reconstruction, and disapproval - Basis of deisgn, actions, and resistances", Koninklijk Nederlands Normalisatie Instituut, Netherlands, 2020.

[6] P. A. Cundall, "A computer model for simulating progressive, large-scale movements in blocky rock systems", Proceedings of the International Symposium on Rock Mechanics, 8, 129–136, 1971.

[7] Itasca Consulting Group Inc., "3DEC - Three Dimensional Distinct Element Code, Ver. 7.0.", Itasca, 2020.

[8] S. Jafari, J. G. Rots, R. Esposito, "A correlation study to support material characterisation of typical Dutch masonry structures", Journal of Building Engineering, 45, 1–14, 2022, DOI: 10.1016/j.jobe.2021.103450.

[9] G. R. Frazee, "New Formulations of Boussinesq Solution for Vertical and Lateral Stresses in Soil", Practice Periodical on Structural Design and Construction, 26, 1-12, 2021, DOI: 10.1061/(asce)sc.1943-5576.0000567.11